Journal of Data Acquisition and Processing
ISSN: 1004-9037
https://sjcjycl.cn/
DOI: 10.5281/zenodo.777324

ANFIS BASED MPPT AND CASCADED H-BRIDGE, 31-LEVEL MLI WITH HIGH GAIN LANDSMAN CONVERTER IN SINGLE-PHASE SPV POWER WITH GRID CONNECTIVITY FOR IMPROVING POWER QUALITY.

Naresh Kumar
Asstt. Prof, EES University Poly.,F/o Engg. & Technology, Jamia Millia Islamia, New Delhi-India, nkumar2@jmi.ac.in

Anwar Shahzad Siddiqui
Prof., D/o Elect. Engg., F/o Engg. & Technology, Jamia Millia Islamia, New Delhi-India
assiddiqui@jmi.ac.in

Rajveer Singh
Asso. Prof., D/o Elect. Engg., F/o Engg. & Technology, Jamia Millia Islamia, New Delhi-India rsingh@jmi.ac.in

Abstract
The use of solar PV systems as a cost-effective and popular renewable energy generation system has gained widespread attention in recent years. To maximize a PV module's power output, various control techniques are utilized. For arbitrary electric loads, it has been proven that the ANFIS-based MPPT approach offers better results. The Landsman converter is a critical component in this paper that optimizes dc voltage of small level from PV panel and produces a constant dc link voltage for grid through the inverter. A 1-phase thirty-one level cascaded asymmetrical MLI is utilized in this paper, producing wave forms of staircase-like structure and many output levels while using fewer system components to achieve minimal THD values. An ANN algorithm is utilized to update the PI parameters to achieve excellent results under varying operating points. The proposed controller improves power quality by providing grid synchronization and excellent reference tracking. MATLAB/Simulink software is used to model the entire process, which helps to validate the proposed system's control performance. Overall, the use of anfis-based mppt technique &landsman converter, along with a single-phase 31-level asymmetrical cascaded MLI and ANN-based PI controller, is an efficient and effective method of generating renewable energy with high power quality and low THD values.

Key words: PV module, ANFIS based MPPT, ANN and PI Controller

I. Introduction

Environmental pollution is one of the major threat factors that is to be controlled immediately since it causes certain health issues in human beings. With this concern, clean and ecologically responsible energy generation is the most preferred one as it promotes sustainable energy generation that accelerates the social change and improves the living standard [1]. On the other hand, cost factor is the major critical aspect for any technology's success or failure. By considering the above-mentioned criteria, the most viable, pollution free solar PV energy generation system has been utilized as an alternative option for traditional power generation.

The PV system has been categorized as standalone and grid integrated in which grid connected PV is widely in practice as it promotes feasible energy generation[2]. To enhance the low-level DC voltage source, the DC-DC converter is employed as it offers a variety of input as well as output voltage shift ratio, quick current and voltage control. There are several DC-DC converters available in an electronic market to step up the DC voltage gain as per the requirement. Among all, the most common is the boost converter because it may be utilized for a variety of high voltage applications [3]-[4].

The high duty rate process of traditional boost designs is the primary cause of inefficiency and the non-ideal resistance in the converter device causes dissipative losses [5]. The pitfalls with boost converter allow us to employ buck boost converter as it has the ability to perform both buck and boost operation. The electrical power is shifted from HV to LV port in buck mode whereas in boost mode it gets shifted from LV to HV port. A basic buck-boost converter performs step-up &step-down operations but unable to obtain optimum voltage gain due to non-continuous input current [6]-[7]**.**In contrast to boost and buck boost converters, the presence of an inner capacitor in CUK converter engaged in transferring the energy which brings out better solution. The CUK converter produces self-balancing output voltage that removes the switching stress of device**.** However, the CUK converter suffer due to poor efficiency and the presence of enormous switching components makes the device bulky and costly to implement. The drawback of the CUK converter is rectified by adopting SEPIC converter as it offers stable operation by eliminating transient undershoots and overshoots whereas the zeta converter comprises lower output voltage ripple and better compensation compared to SEPIC converter [8]-[10**].** However, to improve the efficiency and attaining peak value of voltage gain, the LUO converter is suitable. The output voltage of the LUO converter is stable enough to verify the effectiveness of charging in both a steady state and a voltage-varying condition. Though it generates high energy, it has some disadvantages like high-cost efficiency, induces current and voltage stress [11]. In this study, the Landsman converter was suggested in order to address the drawbacks of the aforementioned converters to improve the switching performance and accomplish the maximum voltage gain value.

The major challenge is to integrate the energy sources which vary in magnitude due to change in weather condition. The MPPT technique has been assigned to overcome this issue as it enhances system efficiency by monitoring the maximum power point of the PV source. Several MPPT techniques are in practice which help in obtaining the supreme constant power by trailing the required MPP has been provided in the literature. The P&O (perturb and observe) is a popular algorithm. On the other hand, Incremental Conductance (INC) technique is utilized as a better alternative to P&O in MPPT operation. But these algorithms display oscillations at MPP condition and the balance between dynamic response and steady state accuracy is needed to determine the optimal phase size for MPPT operation. Other traditional MPPT methods have been implemented effectively having less complexity. However, these classical MPPT techniques ignore the impact of partial shading and fail to monitor the target MPP [12].Therefore, AI Artificial Intelligence) based MPPT techniques including FLC (Fuzzy Logic Control) MPPT and ANN (Artificial Neural Network) based MPPT approaches have been adopted to address the aforementioned problems.FLC [13] is an eye-catching technique because it doesn’t need machine learning experience in order to incorporate MPPT and also it

has a simplified configuration and robust design that helps to overcome the PV power system's uncertainty and non-linearity issues. But prime challenge of utilizing fuzzy logic MPPT is of requiring expert knowledge and the rule-based system design. On the other hand, for quick power tracking under changing environmental conditions, ANN based MPPT comprised of multilayer neurons is widely adopted. However, large quantities of data are needed for proper training which is performed on a regular basis to obtain an accurate MPPT using this approach [14]. The hybrid algorithm has been proposed in this paper which combines ANN and FLC with attracting learning abilities that include qualified membership for MPPT action.

Because of this, the converter produces the DC-link voltage that acts as input for inverter. Even though a dc-ac inverter is required, the multilayer inverter (MLI) is currently preferred over the conventional voltage source inverter (VSI) since it can produce high-quality electricity with little error. A single phase, 31-level cascaded multilevel inverter has been used in this requirement and is ideal for solar power and commercial applications [15, 16]. A PI controller is used to control the inverter's performance because it maintains sinusoidal output current, offers outstanding dynamic efficiency under regularly changing environmental conditions, and helps to attain unity power factor [17]. It usually takes too long to solve the optimization problem using the PI controller [18], so a rapid and trustworthy approach is preferred to address the optimization problem. As a result, the fuzzy logic control method has been used since it is the most familiar with control system design and does not anticipate the mathematical model. Additionally, it controls both linear and non-linear PV systems using language principles, which form the cornerstone of human logic. However, the FLC algorithm's effectiveness is entirely dependent on the membership functions, which require time to develop [19, 20]. In order to get better results, a PI controller based on an ANN algorithm has been presented in this research to address this issue.

The PWM generator transfers the PI controller's output to the inverter, which controls output voltage, lowers overall THD, and enhances power quality. After performing harmonic reduction and power factor compensation in the line current, the multilayer inverter delivers active power to the grid [21]. The grid is synchronized [22] using a PLL to achieve active power exchange, improve power quality, and increase system reliability.

The research on PV system power generation is organized in the proposed work using a landsman converter for high power output and an ANFIS algorithm-based MPPT assigned to follow the maximum power point from the PV module. The overall efficiency is raised by using a 31-level cascaded inverter, which produces high-quality output. To regulate the voltage sent to the grid, an ANN-based PI controller is used with the inverter. As a result, the following sections will examine the modelling of PV systems, landsman converters with ANFIS MPPT control schemes, ANN-based PI controllers, and 31-level inverters.

II. Proposed Control Scheme

The PV panel, which transforms solar energy into electrical energy, serves as the system's power source. The ANFIS-based MPPT controller tracks the PV panel's maximum power point and modifies the operating point to maximize power production using ANFIS system (Adaptive Neuro-Fuzzy Inference System). A complex algorithm, ANFIS-based MPPT, can monitor the MPP more precisely compared to traditional techniques. The Landsman Converter

is a sort of dc-dc boost converter which raises the output voltage of PV panel to a level that can be fed into the inverter. To attain great efficiency, the Landsman Converter uses a linked inductor and dc-link capacitor is used to stabilize the inverter's input and filter the DC voltage. An ANN-based proportional integral controller manages the voltage at output and current of a 31-level multi-level inverter by modelling the dynamics of the system with ANN and implementing a Proportional-Integral (PI) control algorithm. The measurements of output V & I along with the current system status, are inputs to the ANN in an ANN-based PI controller. Following the processing of these inputs by the ANN, the output V& I of the inverter are adjusted up to desired set points by computing the necessary control signals. The PI controller modifies the control signals on the bases of difference in error between the required and actual values of V & I. One advantage of utilizing an ANN-based PI controller to manage the output V & I of a 31-level multi-level inverter is its ability to handle the intricate and highly nonlinear dynamics of the system. Moreover, ANNs have the capacity to learn and adjust to shifting system parameters, which can enhance inverter performance and stability. It is crucial to remember that in order to develop an ANN-based PI controller for a 31 level multi-level inverter, significant computational resources and training data may be needed. Moreover, specific knowledge in both power electronics and machine learning may be needed for the design and implementation of such a controller.

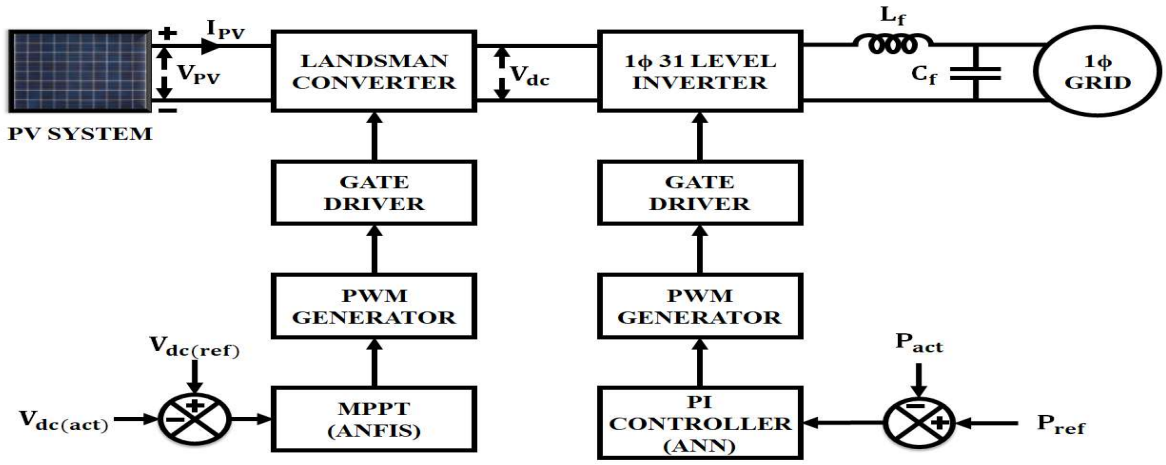

Fig. 1 Proposed control block of PV system with LM Converter and 31-level Inverter.

Whole, a sophisticated system that needs careful design and tuning is the control block scheme of a PV system with landsman converter and 31-level inverter with ANFIS-based MPPT. By using advanced control techniques and high-quality components, designers can achieve high efficiency and reliable operation under a variety of operational circumstances. The ANFIS-based MPPT algorithm provides accurate and efficient tracking of the MPP, improving the overall system performance. Complete, an ANN based PI controller for regulating the output V & I of a 31-level multi-level inverter is a powerful tool that can improve the performance and stability of complex power electronics systems.

III. Modeling of the Suggested Control Scheme

A. Modeling of SPV System

Semiconductor material in the cell absorbs photons of light that excite the electrons and cause them to move when they hit the cell. Electric current is produced by this flow of moving electrons and can be used to power electrical appliances. The separation of the electrons and holes produced by light absorption is carried out by the cell's p-n junction diode. A potential difference or voltage is produced across the cell by the junction's inherent electric field, which causes the electrons and holes to travel in opposing directions. A PV cell's output voltage is in direct proportion to the amount of light it receives. Voltage produced by the cell increases with the light intensity. Normally, the voltage of a single cell is a few hundred milli volts**.** A solar panel composed of many series-connected PV cells to increase the voltage and power output of the PV system. Solar panel voltage is determined by adding the individual cell voltages together, and the panel's power output is determined by multiplying its generated voltage by its produced current. Figure 2 shows a PV cell's electrical configuration.

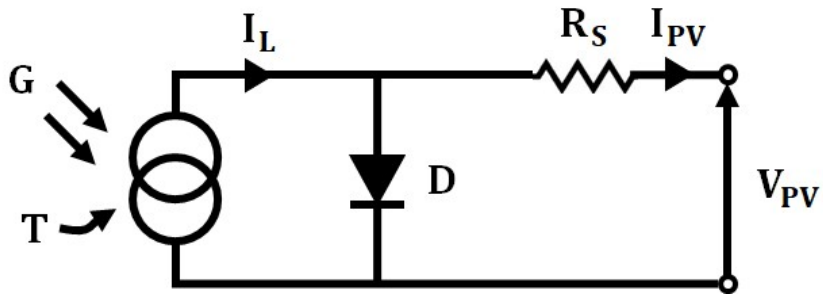

Fig. 2 Electrical Layout of the PV cell

The expressions for the relationship between the PV cell's output voltage and current are given as,

$$I_{PV} = I_L - I_0\left[e^{\frac{q(V_{PV}+I_{PV}+R_S)}{nkT}} - 1\right] \quad (1)$$

$$I_L(G,T) = I_{cc}\frac{G}{1000}\left[1 + a(T - T_{ref})\right] \quad (2)$$

$$I_0(T) = I_0(T_{ref}).\left(\frac{T}{T_{ref}}\right)^{\frac{a}{n}}.e^{\frac{-q.Eg}{n}\left(\frac{1}{T}-\frac{1}{T_{ref}}\right)} \quad (3)$$

$$I_0(T_{ref}) = \frac{I_{cc}}{e^{\frac{qV_{oc}}{nkT_{ref}}}-1} \quad (4)$$

$$R_s = \frac{dV_{PV}}{dI_{PV}}\Big|\, V_{oc} - \frac{nkT}{I_{cc}qe^{\frac{qV_{oc}}{nkT_{ref}}}} \quad (5)$$

Where G stands for solar irradiation, T for temperature, K for plank's constant I_o for saturation current, I_L for photo current, Rs for series resistance, Rp for shunt resistance, I_{PV} for output current of PV cell and V_{PV} for the cell's output voltage. The equivalent circuit model of PV cell is comprised of a current source, a diode, a series resistance and a shunt resistance. The diode equation that considers solar radiation, temperature, saturation current, and other factors, relates the output V & I of the SPV cell. The output V & I are decreased and losses are introduced by the series and shunt resistances, which also have an impact on the PV cell's performance.

B. LM Converter Model

The design of papering of Landsman converter in a continuous current conduction mode regardless of change in the level of irradiation is depicted in Fig. 3. There are two operating modes of converter circuit.

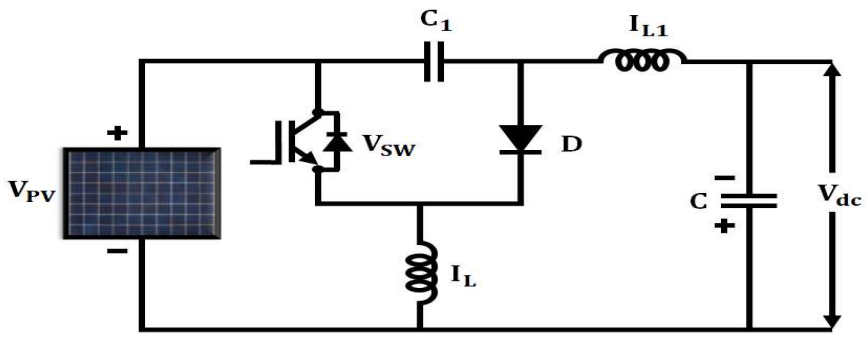

Fig. 3 Electrical Layout of LM Converter

Mode 1: Switch ON Mode

As the switch in Mode-1 is switched ON, reverse-biased diode allows the current to flow from the inductor through the switch. Because capacitor C_1 voltage(V_{C1}) becomes higher than DC input voltage (V_{dc}) and capacitor C_1 charges L and the output. The voltage across the inductor (V_L) increases as the current (I_L) through inductor increases. Fig. 4 illustrates the reduction in V_{C1} as a result of this the inductor L_1 receives energy from the input and this energy is then stored as magnetic energy in the inductor. In the next mode, the output receives the energy that inductor L1 has stored (Mode 2).

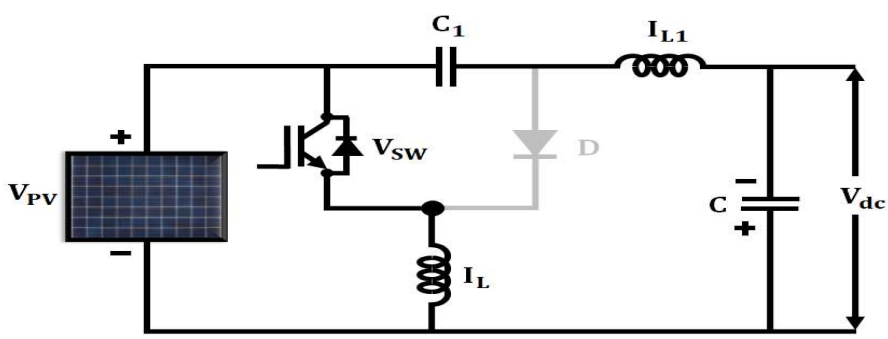

Fig. 4 Circuit of LM converter with Switch ON mode

Mode 2: Switch OFF Mode

Fig. 5 illustrates the diode's forward bias when the switch is off. The diode acts as a conduit for the inductor current I_L. Since capacitor C_1 is charged due to input current and the inductor current I_{L1}, diode is used to transmit the charge that is stored in the inductor L to the output. As a result, V_{C1} increases but I_L decreases.

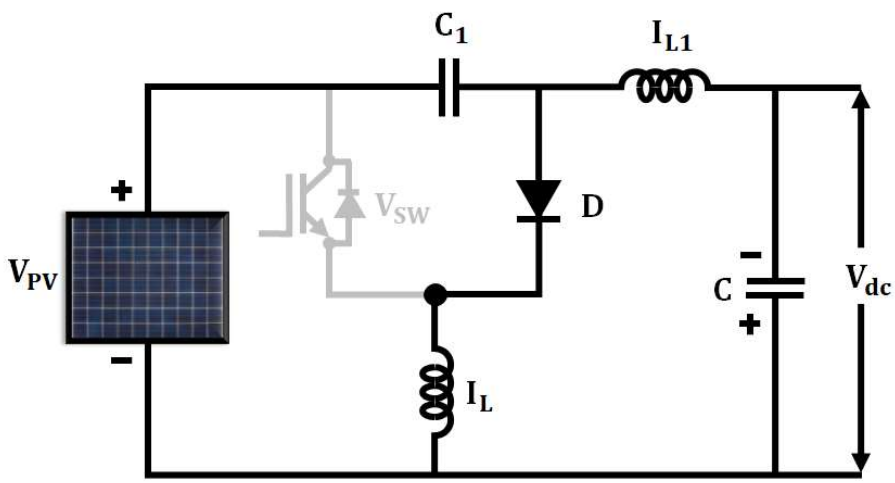

Fig. 5 Circuit Layout of LM Converter in Switch OFF Mode

The ripple current (peak-to-peak) in L_1 is given as,

$$\Delta I_{L1} = \frac{\Delta\phi}{L_1} = \frac{1}{L_1} * \frac{1}{2} * \frac{\Delta V_{C1}}{2} * \frac{T}{2} \quad (6)$$

The value of current through capacitor C_1 while switch is OFF,

$$I_{C1} = I_{L1} = C_1 \frac{\Delta V_{C1}}{(1-D)T} \quad (7)$$

Where, D refers to duty ratio, T represents the switching time.

The voltage ripple at the capacitor C_1 is given as,

$$\Delta V_{C1} = \frac{I_{L1}}{C_1}(1-D)T \quad (8)$$

$$\Delta I_{L1} = \frac{1}{L_1} * \frac{1}{2} * \frac{I_{L1}}{2C_1}(1-D)T\frac{T}{2} \quad (9)$$

$$\Delta I_{L1} = \frac{1}{8L_1C_1}\frac{I_{L1}(1-D)}{f_{SW}^2} \quad (10)$$

Where, f_{SW} is the switching frequency and is given as,

$$f_{SW} = \frac{1}{T}$$

$$I_{L1} = \frac{D}{(1-D)} I_{dc} \quad (11)$$

Where, I_{dc} represents the current (output) of Landsman converter. The value of Inductor L_1 is expressed as follows,

$$L_1 = \frac{DI_{dc}}{8f_{SW}^2 C_1 \Delta I_{L1}} \quad (12)$$

C. ANFIS-Based Max. Power Point Tracking

ANFIS MPPT design consists considering six input layers with two parameters. Three membership functions exist for each input parameter, and they are trained using the ANFIS technique. 9-fuzzy rules can be derived after mapping the input output data sets which help extracting maximum power output. It papers by assigning two inputsI_1 and I_2that are either half the MF distribution's base width or the base width for triangular MF distributions. Each input has three neurons and the nine fuzzy rules are the outcome. Thus, the output y_i based on Takagi and surgeon FLC model is given as follows,

$$y_i = a_i I_1 + b_i I_2 + c_i \quad (13)$$

Where, I_1 denotes the number of fuzzy rules, $a_{i,} b_i \; and \; c_i$ are the output equation coefficients.The normalized value V_{1avg} , which lies in the range [0,1] are the weights connecting these layers and is mainly depending on the triangle membership distribution function's base width. Therefore, it can be expressed as,

$$V_{1\,avg} = \frac{V_{11}+V_{12}+V_{13}}{3} \quad (14)$$

$$V_{2\,avg} = \frac{V_{24}+V_{25}+V_{26}}{3} \quad (15)$$

Where, V_{11}represents the weight that links the 1st node in layer-1 with 1st node in layer-2, V_{12} interconnects 1st node in layer-1 with the second node in layer-2& so on.

According to the formula w_n = firing power, the best optimized value of each fuzzy rule is chosen or fired. The letter N designates the node that does the normalization. As a result, the firing strength's normalized value is given as,

$$w_{1\,out} = \frac{w_1}{(w_1+w_2+\cdots+w_9)} \quad (16)$$

The MF distribution of input variables has an impact on the performance of ANFIS. a_i , $b_i \; and \; c_i$ are the optimal parameter values are chosen carefully, so that ANFIS performs at its best. Thus, the prediction has been made accurately. The dynamic response of this technique is sufficiently high particularly when SPV power is connected to the grid and system stability is maintained. Figure 6 portrays the ANFIS based MPPT flow chart.

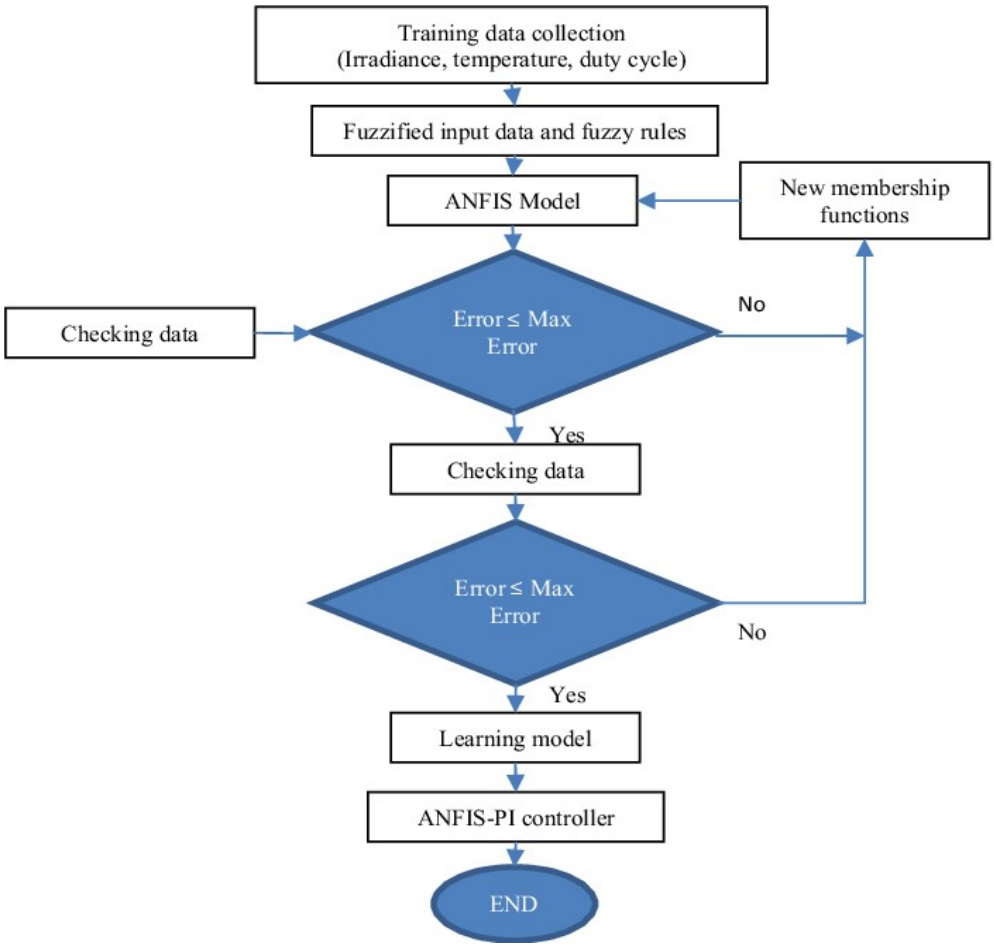

Fig. 6 Hybrid ANFIS-MPPT Flow Chart

Collect the two input-output datasets from the PV module initially while it is exposed to various weather conditions. These data sets serve as the ANFIS technique's training examples. When the data sets are trained with sufficient iterations, it can improve the input output mapping of the data sets. To generate appropriate output for a range of input values, ANFIS modifies the membership function (MF) values to produce a set of fuzzy rules. The parameters of the MF are adjusted or changed before minimizing the mistake. Once all the parameters of the membership function have been changed, the ANFIS model is transformed into a learning model that is used in the MPPT control strategy. Prior to employing the hybrid ANFIS approach for MPPT power, the results are confirmed by comparison with the checking data, which is distinct from the training data. If the error produced exceeds the desired value, change the MF parameters to bring the error down. The dc-dc converter is made to appear as though it is installed between the PV module and the inverter by altering the Landsman converter's duty cycle.

D. Modeling of 31-Level Inverter

In high and medium power applications, MLI is commonly used. The Cascaded H-Bridge (CHB), the Neural Point Clamped (NPC), and the Flying Capacitor (FC) Inverters are three different types of MLIs. The CHB inverter is chosen among these topologies because of its

simple design, flexibility and ability to interact with renewable energy resources. Based on the size of the dc voltage source, CHB inverters are classified as either symmetrical or asymmetrical inverters.

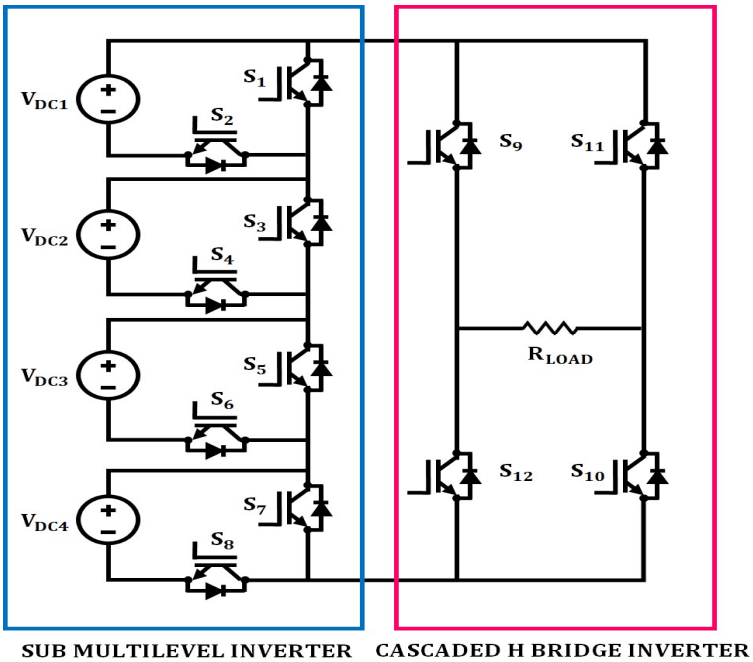

Fig. 7 A 31-Level Asymmetrical cascaded MLI

The input voltage source in a symmetrical CHB MLI has the same magnitude. If there are "N" connected H-bridges, then the output voltage can reach "M" levels, where M=2N+1 is the number of levels. Therefore, a symmetrical CHB MLI employs fifteen H-bridges for generating a thirty-one-level stepped voltage waveform at the output. Ratio of magnitudes (input dc voltage source) in asymmetrical CHB MLI is given as V_{dc1}:V_{dc2}:V_{dc3}:V_{dc4}=1:2:4:8, is used to generate 31 levels. Thus, the relation for asymmetrical MLI is given as M = (2Nx2)-1. Where, M denotes the maximum level (in output voltage waveform), N represents the number of H-bridges.

An asymmetrical CHB MLI generates a 31-level output waveform with just 8 MOSFET switches and 4 power diodes. As a result, asymmetrical design is favored because it requires fewer components to achieve higher peak voltage levels. Consequently, switching losses are significantly reduced. The input voltages are $V_{dc1} = 13V, V_{dc2} = 26V, V_{dc} = 52V, V_{dc4} = 104V$. Thus, the inverter output voltage is given below table. The sine and dc offset waves generate the switching pulses for gate which are given to the logic gate circuit to produce PWM for the switches.

Table-1, 31-Level MLI Switching Table

Inverter V_{output}	**S_1**	**S_2**	**S_3**	**S_4**	**S_5**	**S_6**	**S_7**	**S_8**	**S_9**	**S_{10}**	**S_{11}**	**S_{12}**
$15\,V_{dc}$	1	0	1	0	1	0	1	0	1	1	0	0
$14\,V_{dc}$	0	1	1	0	1	0	1	0	1	1	0	0
$13\,V_{dc}$	1	0	0	1	1	0	1	0	1	1	0	0
$12\,V_{dc}$	0	1	0	1	0	1	1	0	1	1	0	0
$11\,V_{dc}$	1	0	1	0	0	1	0	1	1	1	0	0
$10\,V_{dc}$	0	1	1	0	0	1	0	1	1	1	0	0
$9\,V_{dc}$	1	0	0	1	1	0	0	1	1	1	0	0
$8\,V_{dc}$	0	1	0	1	1	0	0	1	1	1	0	0
$7\,V_{dc}$	1	0	1	0	1	0	1	0	1	1	0	0
$6\,V_{dc}$	0	1	1	0	0	1	1	0	1	1	0	0
$5\,V_{dc}$	1	0	0	1	0	1	1	0	1	1	0	0
$4\,V_{dc}$	0	1	0	1	0	1	1	0	1	1	0	0
$3\,V_{dc}$	1	0	1	0	1	0	0	1	1	1	0	0
$2\,V_{dc}$	0	1	1	0	1	0	0	1	1	1	0	0
$1\,V_{dc}$	1	0	0	1	1	0	0	1	1	1	0	0
$0\,V_{dc}$	0	0	0	0	0	0	0	0	0	0	1	1
$-1\,V_{dc}$	1	0	0	1	0	1	0	1	0	0	1	1
$-2\,V_{dc}$	0	1	1	0	0	1	1	0	0	0	1	1
$-3\,V_{dc}$	1	0	1	0	0	1	1	0	0	0	1	1
$-4\,V_{dc}$	0	1	0	1	1	0	1	0	0	0	1	1
$-5\,V_{dc}$	1	0	0	1	1	0	1	0	0	0	1	1
$-6\,V_{dc}$	0	1	1	0	1	0	0	1	0	0	1	1
$-7\,V_{dc}$	1	0	1	0	0	1	0	1	0	0	1	1

$-8\,V_{dc}$	0	1	0	1	0	1	0	1	0	0	1	1
$-9\,V_{dc}$	1	0	0	1	0	1	0	1	0	0	1	1
$-10\,V_{dc}$	0	1	1	0	1	0	1	0	0	0	1	1
$-11\,V_{dc}$	1	0	1	0	1	0	1	0	0	0	1	1
$-12\,V_{dc}$	0	1	0	1	1	0	1	0	0	0	1	1
$-13\,V_{dc}$	1	0	0	1	0	1	1	0	0	0	1	1
$-14\,V_{dc}$	0	1	1	0	0	1	0	1	0	0	1	1
$-15\,V_{dc}$	1	0	1	0	0	1	0	1	0	0	1	1

PWM Modulation

The carrier signal has a 10 kHz switching frequency and is compared to the reference sinusoidal signal. This switching frequency has been chosen to minimize inductance size and switching loss, which is important for low-power converters. The goal is to keep the switching frequency below 100 kHz, which doesn't require a complex layout. To generate the reference signal, an ANN-based PI controller is employed. The H-bridge inverter, which operates at the standard frequency of 50 Hz, receives sinusoidal 180-degree PWM conduction pulses. The use of PWM technique helps to reduce the harmonic distortion of the output waveform that improves the efficiency of overall system. The PWM has been adopted to remove the prevailing third order harmonics. Therefore, the amplitude modulation and the frequency modulation can be expressed as,

$$M_a = {A_{mod}}/{A_{carr}} \tag{17}$$

$$M_f = {f_{carr}}/{f_{mod}} \tag{18}$$

E. ANN based PI Controller for Grid

PI controller is mainly used for parameter tuning and performance control applications and it helps in regulating the DC-link voltage that is injected into the grid.

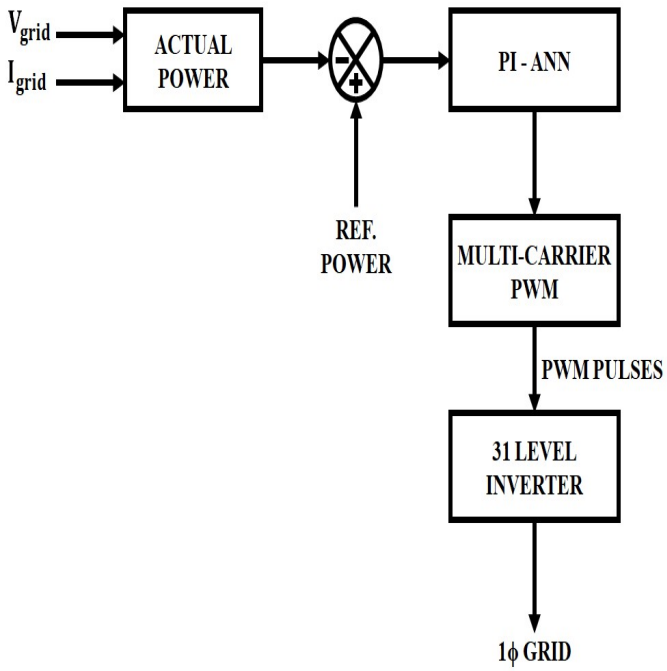

Fig. 8 Grid synchronization using ANN based PI controller.

The nth sampling instant error voltage is expressed as

$$\Delta v_{err}(n) = v_{dc}^{*}(n) - v_{dc}(n) \quad (19)$$

The PI controller output at n^{th} sampling instant can be expressed as

$$i_{inv}^{*}(n) = i_{inv}^{*}(n-1) + K_{P1}\left(\Delta v_{err}(n) - \Delta v_{err}(n-1)\right) + K_{I1}\Delta v_{err}(n) \quad (20)$$

An ANN based PI controller for regulating the output V & I of a 31-level MLI involves using an Artificial Neural Network for modeling the system dynamics and implement a Proportional-Integral control algorithm to adjust the inverter's output V & I. Artificial Neural Network based PI controller takes the current system state, such as the output V & I measurements, as inputs for ANN**.** Then ANN processes these inputs and calculates the appropriate control signals to adjust the inverter's V & I output upto the desired set points. The PI controller modifies the control signals based on the difference in error between the desired voltage and actual voltage and current values. The PI controller uses the error signal between the actual and desired voltage and current values to adjust the control signals. One of the benefits of using an ANN based PI controller for regulating the output V & I of a 31-level MLI is that it can handle the complex and highly non-linear dynamics of such a system. Additionally, ANNs can learn and adapt to changing system conditions, which can lead to better performance and stability in the inverter control**.** However, the implementation of an ANN based PI controller for a 31 level multi-level inverter may require significant computational resources and training data to achieve accurate and stable control. Additionally, the design and implementation of such a controller may require specialized expertise in both power electronics and machine learning. Overall, an ANN based PI controller for regulating the output V & I of a 31-level MLI is a

powerful tool that can improve the performance and stability of complex power electronics systems.

IV. Results and Discussions

The solar panel has a total of 10 modules, each consisting of 36 series-connected cells, with an area of 125mm x 31.25mm per cell. The PV panel operating voltage is 16.8V, the maximum voltage is 1000V DC. The operating current of the panel is 5.8A, and the temperature rating is from -40°C to +85°C.These specifications are important for calculating the MPP of the PV panel and determining the efficiency of the overall system. The MPP is a point where the PV panel operates at maximum efficiency, and it is calculated by finding the V & I at which the panel produces the maximum output power. The temperature rating is also important, as the efficiency of the panel becomes poor when the temp.rises. Landsman converter is a dc-dc converter that converts the output of the solar system to a level that is suitable for the load. The converter's input voltage ranges from 0 to 48 V DC, and its maximum input current is 25 A. The capacitances of the converter are C and C_2 and have values of 853µF and 312.7µF, respectively. The inductances of the converter are L and L_2 and have values of 5.45mH and 0.99mH, respectively. The converter's operating frequency is 10kHz, and its output current is 5A.The converter's output power is 700W.These specifications are important to design the converter's control system. Also values of the capacitances and inductances are particularly important to design the converter's control system, as they assess how the converter reacts to variations in input and output voltages and currents. The maximum input current and output power are important for ensuring that the converter can handle the load without being damaged.

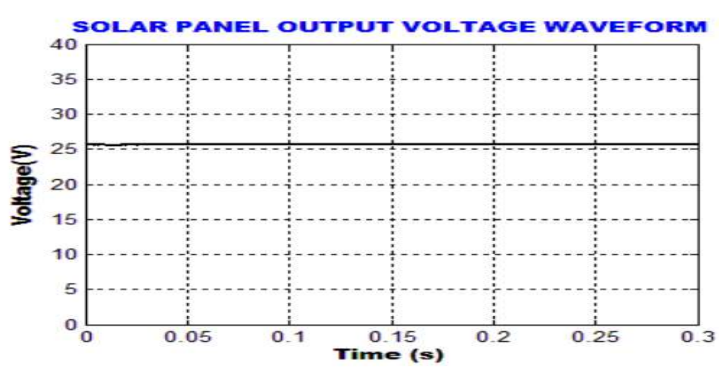

Fig. 9 Solar panel output voltage waveform.

The DC output voltage generated by SPV panel may be small because of solar irradiance. The generated DC voltage of solar panel with respect to time is noted as $26V$ which is clearly shown in Fig. 9.

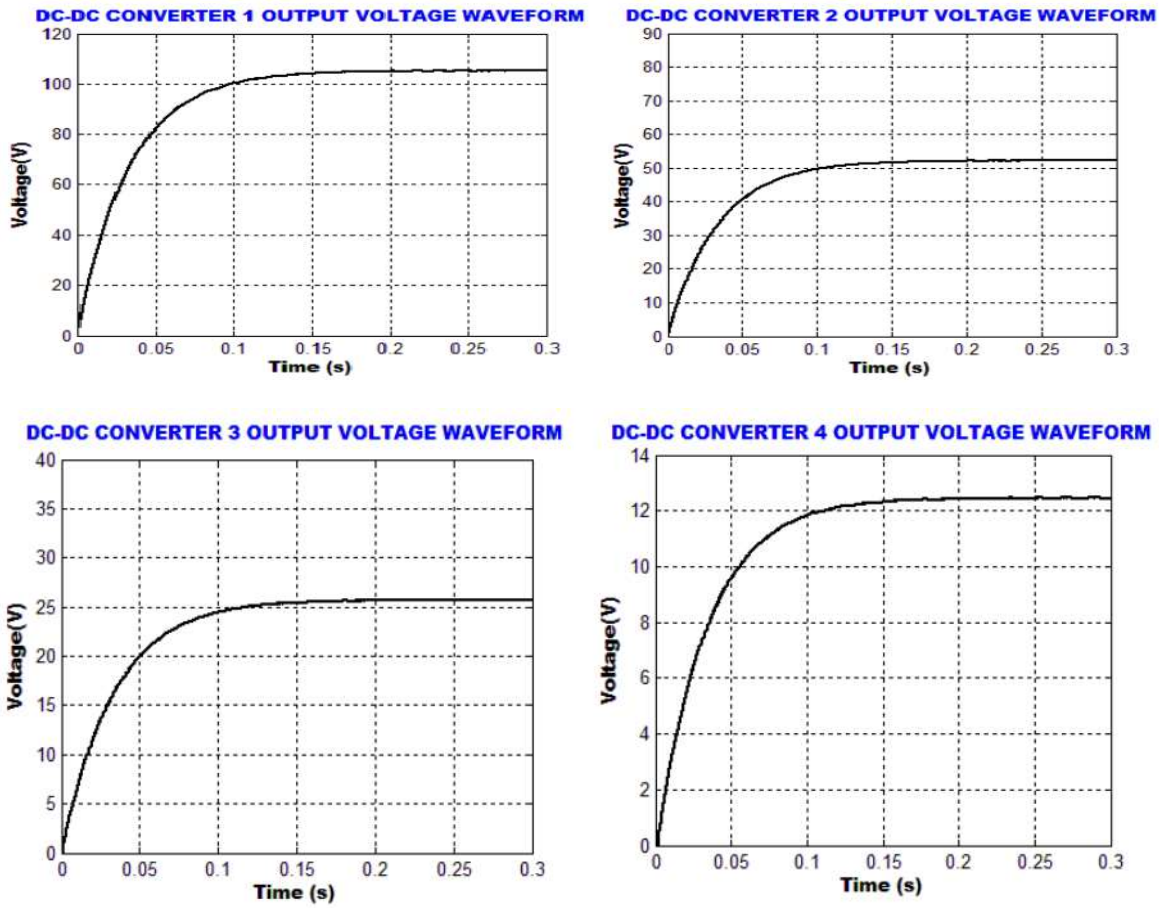

Fig.10 Four-Level Output DC-link voltage of LM Converter

This small output DC voltage produced by the SPV panel is boosted up by utilizing Landsman converter. Thus, the converter generates the DC-link voltage with high transfer voltage gain is applied to the 31-level inverter. To generate 31-levels, converter generates 4 level dc-link voltage in the ratio of 1:2:4:8 which is clearly depicted in Fig. 10.

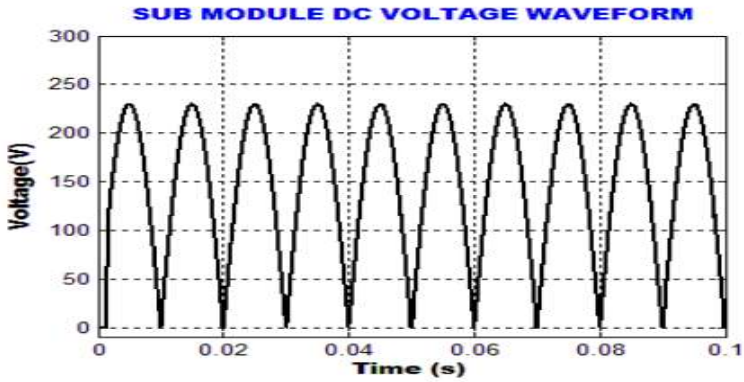

Fig. 11 DC Voltage Waveform of Sub Module

From the waveform depicted in Fig. 11 it is observed that the sub module DC voltage varies between0 $V\ and\ 230V$.

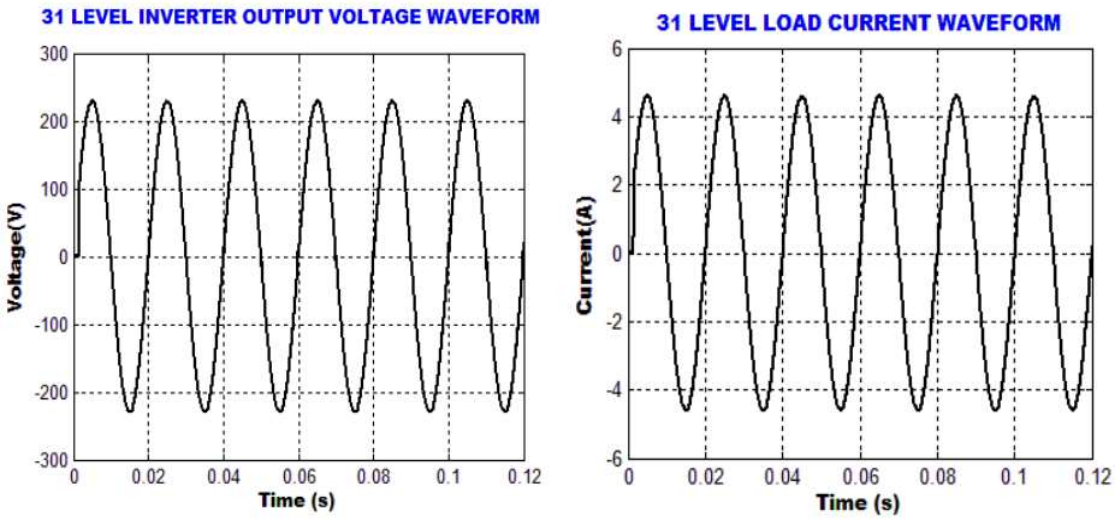

12(a) 12(b)

Fig. 12 waveform of (a) 31-level inverter output voltage (b) 31-level inverter load current

The DC-link voltage produced by the landsman converter is applied to the 31-level inverter. The waveforms of 31-level inverter's output voltage and load current are depicted in Figs. 12(a) & 9(b). Thus, this waveform clearly shows that the inverter's voltage output varies between$-230\ V\ and + 230\ V$. On the other hand, the load current produced by the inverter varies between$-4.3A\ and + 4.3A$ respectively. The output of the inverter is applied to the grid via LC filter which removes the harmonics and noises present in the in the inverter output.

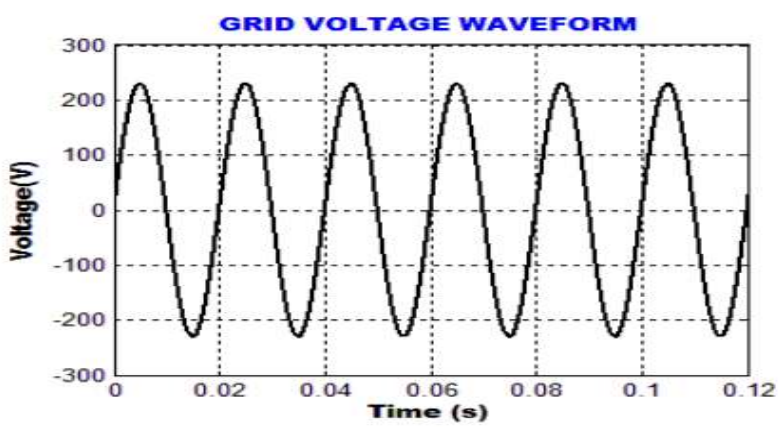

Fig. 13 Grid output voltage waveform

Fig. 13 portrays the voltage output waveform of the grid. The inverter output is applied to the PI controller so the actual and reference values of the real and reactive powers have been analogized and thus the pulses required for the grid are produced by PWM generator. Eventually, the sine wave attained due to LC filter is fed in to the grid.

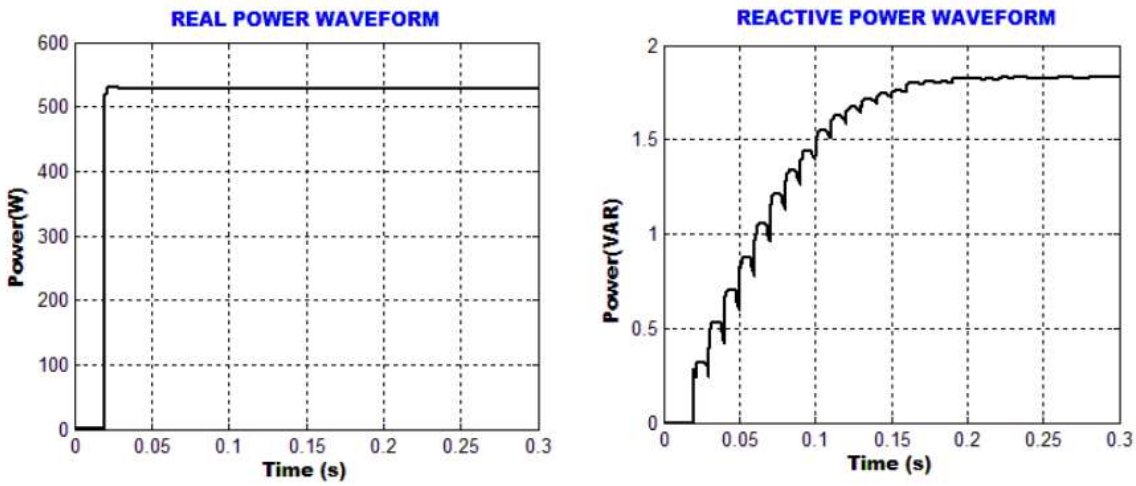

Fig. 14 Wave form of real power and reactive power

The active power deliverance and the reactive power exchange among the grid is controlled by achieving grid synchronization. Fig.14 depicts the real and reactive power waveforms and it is clearly seen that the real power increases initially and it remains constant at 530W. On the other hand, the reactive power gradually rises and maintain its value constant after reaching 1.8A.

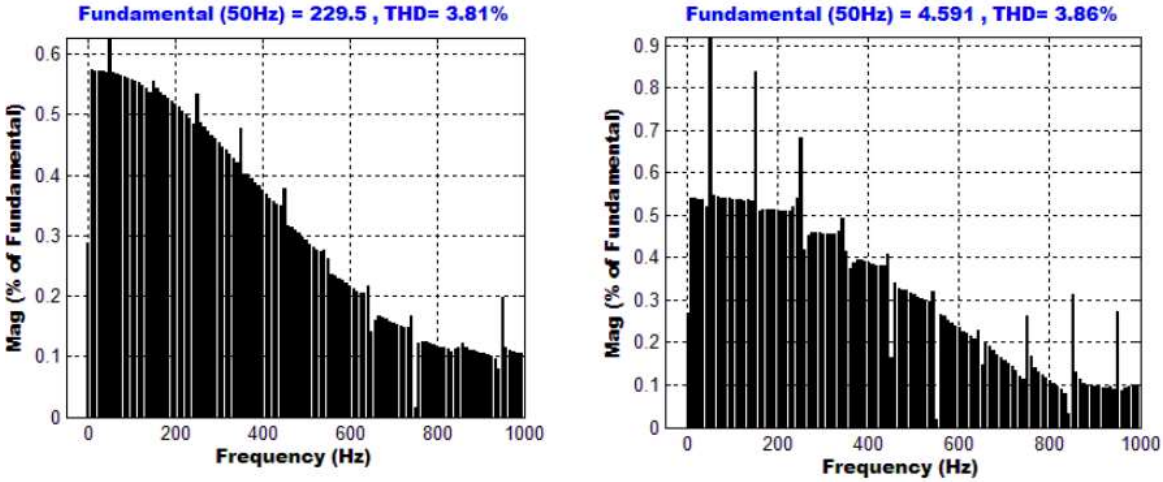

Fig. 15 THD waveform of 31-level inverter (a) output voltage (b) load current

Figs. 15 (a) & (b) depicts the THD waveform of 31 level inverter output voltage and load current. Thus, the above waveform shows that the THD of the proposed system is extremely low and hence the output voltage and load current THD of 31-level inverter is noted as 3.81% and 3.86% respectively.

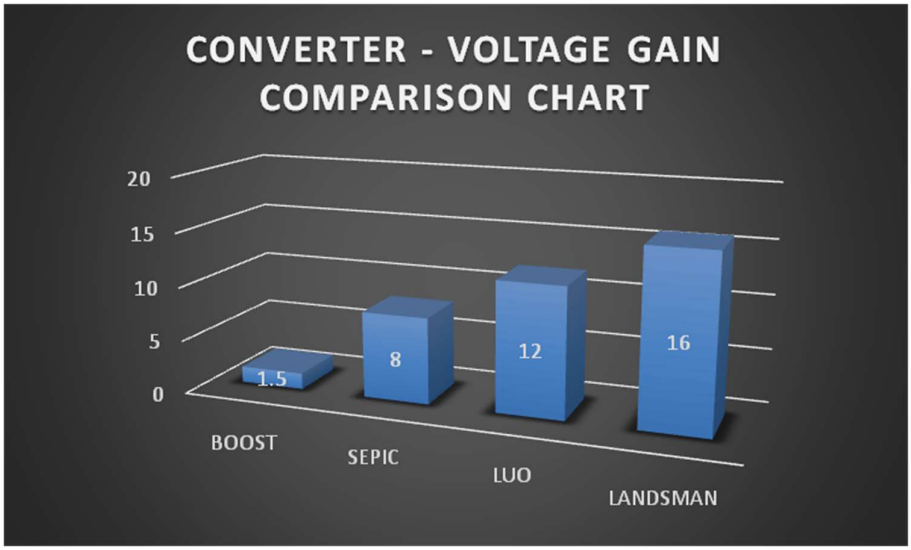

Fig. 16 Voltage gain comparison chart of different converter

Fig. 16 clearly compares the voltage transfer gain value of the Landsman converter with that of other converters with various voltage gain values. The voltage gain ratio of the Landsman converter is extremely high when compared to other converters, and its value is noted as 1:16. In contrast, the voltage transfer gain ratio of the Boost, SEPIC, and LUO converter is relatively low, and its values are given as 1:1.5, 1:8, and 1:12, respectively.

V. Conclusion

This paper analyses the overall control performance and steady state behavior of the PV system with Landsman converter using the ANFIS-based MPPT technique. The use of a landsman converter has removed the need for external filtering and helps to damp oscillations occur in the source current from the PV module in which the oscillations are caused by snubber components. Under varying weather conditions, the ANFIS MPPT approach is used to enable effective and efficient tracking of the maximum possible power from PV modules. ANFIS monitors maximum output power without oscillation especially at low irradiance level. At all solar irradiance stages, the proposed MPPT control scheme responds quickly and has a high gain value. The efficiency and functionality of MLI under dynamic load disturbances and steady state condition have been investigated. In terms of stability, response time and reference tracking, the ANN-PI controller has the best dynamic efficiency. Furthermore, the ANN-PI controller dampens the THD of the injected current to ensure supreme power generation.

References

1. Rajvikram Madurai Elavarasan; G.M.Shafiullah; Sanjeevikumar Padmanaban; Nallapaneni Manoj Kumar; Annapurna Annam; Ajayragavan Manavalanagar Vetrichelvan; Lucian Mihet-Popa; Jens Bo Holm-Nielsen, Year: 2020, “A Comprehensive Review on Renewable Energy Development, Challenges, and Policies of Leading Indian States With an International Perspective”, IEEE Access, Vol: 8, Issue: 5, pp: 74432 - 74457.

2. Amresh Kumar Singh; Shailendra Kumar; Bhim Singh, Year: 2020, "Solar PV Energy Generation System Interfaced to Three Phase Grid With Improved Power Quality", IEEE Transactions on Industrial Electronics, Vol: 67, Issue: 5, pp: 3798 - 3808.

3. Rui Li; Fangyuan Shi, Year: 2019, "Control and Optimization of Residential Photovoltaic Power Generation System With High Efficiency Isolated Bidirectional DC–DC Converter", IEEE Access, Vol: 7, pp: 116107 - 116122.

4. Kumaran Nathan; Saikat Ghosh; Yam Siwakoti; Teng Long, Year: 2019, "A New DC–DC Converter for Photovoltaic Systems: Coupled-Inductors Combined Cuk-SEPIC Converter", IEEE Transactions on Energy Conversion, Vol: 34, Issue: 1, pp: 191 – 201.

5. Mummadi Veerachary; Nikhil Kumar, Year: 2019, "Analysis and Design of Quadratic Following Boost Converter", IEEE Transactions on Industry Applications, Vol: 56, Issue: 6, pp: 6657 - 6673.

6. Mummadi Veerachary; Vasudha Khubchandani, Year: 2019, "Analysis, Design, and Control of Switching Capacitor Based Buck–Boost Converter", IEEE Transactions on Industry Applications, Vol: 55, Issue: 3, pp: 2845 - 2857.

7. Hyeon-Seok Lee; Jae-Jung Yun, Year: 2019, "High-Efficiency Bidirectional Buck–Boost Converter for Photovoltaic and Energy Storage Systems in a Smart Grid", IEEE Transactions on Power Electronics, Vol: 34, Issue: 5, pp: 4316 - 4328.

8. B. R. Ananthapadmanabha; Rakesh Maurya; Sabha Raj Arya, Year: 2018, "Improved Power Quality Switched Inductor Cuk Converter for Battery Charging Applications", IEEE Transactions on Power Electronics, Vol: 33, Issue: 11, pp: 9412 - 9423.

9. Pawan Kumar; Rajeev Kumar Singh; Ranjit Mahanty, Year: 2021, "Performance of MPPT-Based Minimum Phase Bipolar Converter for Photovoltaic Systems", IEEE Transactions on Power Electronics, Vol: 36, Issue: 5, pp: 5594 - 5609.

10. António Manuel Santos Spencer Andrade; Mário Lɐcio da Silva Martins, Year: 2017, "Quadratic-Boost With Stacked Zeta Converter for High Voltage Gain Applications", IEEE Journal of Emerging and Selected Topics in Power Electronics, Vol: 5, Issue: 4, pp: 1787 - 1796.

11. Radha Kushwaha; Bhim Singh, Year: 2019, "A Modified Luo Converter-Based Electric Vehicle Battery Charger With Power Quality Improvement", IEEE Transactions on Transportation Electrification, Vol: 5, Issue: 4, pp: 1087 - 1096.

12. Ratnakar Babu Bollipo; Suresh Mikkili; Praveen Kumar Bonthagorla, Year: 2021, "Hybrid, optimal, intelligent and classical PV MPPT techniques: A review", CSEE Journal of Power and Energy Systems, Vol: 7, Issue: 1, pp: 9 - 33.

13. Neeraj Priyadarshi; Sanjeevikumar Padmanaban; Jens Bo Holm-Nielsen; Frede Blaabjerg; Mahajan Sagar Bhaskar, Year: 2020, "An Experimental Estimation of Hybrid ANFIS–PSO-Based MPPT for PV Grid Integration Under Fluctuating Sun Irradiance", IEEE Systems Journal, Vol: 14, Issue: 1, pp: 1218 - 1229.

14. C. Dhanamjayulu; G.Arunkumar;B. Jaganatha Pandian; C. V. Ravi Kumar; M. Praveen Kumar; A. Rini Ann Jerin; P. Venugopal, Year: 2019, "Real-Time Implementation of a 31-Level Asymmetrical Cascaded Multilevel Inverter for Dynamic Loads", IEEE Access, Vol: 7, pp: 51254 - 51266.

15. Muhammad Najwan Hamidi; DahamanIshak; Muhammad Ammirrul Atiqi Mohd Zainuri; Chia Ai Ooi; Tarmizi Tarmizi, Year: 2021, "Asymmetrical Multi-level DC-link Inverter for PV Energy System with Perturb and Observe Based Voltage Regulator and Capacitor Compensator", Journal of Modern Power Systems and Clean Energy, Vol: 9, Issue: 1, pp: 199 - 209.
16. JeyrajSelvaraj; Nasrudin A. Rahim, Year: 2009, "Multilevel Inverter For Grid-Connected PV System Employing Digital PI Controller", IEEE Transactions on Industrial Electronics, Vol: 56, Issue: 1, pp: 149 - 158.
17. Miguel E. Vivert; Diego Patino; Rafael Diez, Year: 2021, "Modulation Strategy and Controller for Grid-Tied Trinary Hybrid Multilevel Inverter", IEEE Journal of Emerging and Selected Topics in Power Electronics, Vol: 9, Issue: 1, pp: 539 - 548.
18. Albert Alexander Stonier; Srinivasan Murugesan; Ravi Samikannu; Sampath Kumar Venkatachary; S. Senthil Kumar; Prakash Arumugam, Year: 2020, "Power Quality Improvement in Solar Fed Cascaded Multilevel Inverter With Output Voltage Regulation Techniques", IEEE Access, Vol: 8, pp: 178360 - 178371.
19. Mahammad A. Hannan; Jamal A. Ali; Azah Mohamed; Ungku Anisa Ungku Amirulddin; Nadia Mei Lin Tan; Mohammad Nasir Uddin, Year: 2018, "Quantum-Behaved Lightning Search Algorithm to Improve Indirect Field-Oriented Fuzzy-PI Control for IM Drive", IEEE Transactions on Industry Applications, Vol: 54, Issue: 4, pp: 3793 - 3805.
20. Pablo Cossutta; Miguel Pablo Aguirre; Andrés Cao; Santiago Raffo; María Inés Valla, Year: 2015, "Single-Stage Fuel Cell to Grid Interface With Multilevel Current-Source Inverters", IEEE Transactions on Industrial Electronics, Vol: 62, Issue: 8, pp: 5256 - 5264.
21. Nirmal Mukundan C. M.;Jayaprakash P., Year: 2021, "Realization of Cascaded H-Bridge Multilevel Inverter Based Grid Integrated Solar Energy System With Band Stop Generalized Integral Control", IEEE Transactions on Industry Applications, Vol: 57, Issue: 1, pp: 764 - 773.